

The Influence of Ligand Valency on Aggregation Mechanisms for Inhibiting Bacterial Toxins

Cristina Sisu,^[b, d] Andrew J. Baron,^[a] Hilbert M. Branderhorst,^[f] Simon D. Connell,^[a, c] Carel A. G. M. Weijers,^[d] Renko de Vries,^[e] Edward D. Hayes,^[a, b] Aliaksei V. Pukin,^[d] Michel Gilbert,^[g] Roland J. Pieters,^[f] Han Zuilhof,^{*,[d]} Gerben M. Visser,^[d] and W. Bruce Turnbull^{*,[a, b]}

Divalent and tetravalent analogues of ganglioside GM1 are potent inhibitors of cholera toxin and Escherichia coli heat-labile toxin. However, they show little increase in inherent affinity when compared to the corresponding monovalent carbohydrate ligand. Analytical ultracentrifugation and dynamic light scattering have been used to demonstrate that the multivalent inhibitors induce protein aggregation and the formation of space-filling networks. This aggregation process appears to arise when using ligands that do not match the valency of the protein recep-

tor. While it is generally accepted that multivalency is an effective strategy for increasing the activity of inhibitors, here we show that the valency of the inhibitor also has a dramatic effect on the kinetics of aggregation and the stability of intermediate protein complexes. Structural studies employing atomic force microscopy have revealed that a divalent inhibitor induces head-to-head dimerization of the protein toxin en route to higher aggregates.

Introduction

Cholera and travellers' diarrhoea are still life-threatening diseases in many parts of the world.^[1,2] These diarrhoeal diseases are caused by two protein toxins that share over 80% sequence identity: cholera toxin and *Escherichia coli* heat-labile toxin.^[3] Their AB₅ hetero-oligomeric structures comprise a single toxic A-subunit and a pentameric ring of B-subunits that interact with the cell surface glycolipid ganglioside GM1.^[4] Following adhesion at the cell surface and endocytosis of the protein toxin, the A-subunit covalently modifies the regulatory protein Gs α , which ultimately leads to a large efflux of cellular liquid into the gut. The resulting diarrhoea has been reported to contain concentrations of cholera toxin as high as 10 $\mu\text{g mL}^{-1}$,^[5] this corresponds to a B-subunit concentration of approximately 1 μM . Inhibitors of the B-subunit-GM1 interaction could provide a prophylactic treatment for these debilitating diseases.^[6] It has been shown that compounds bearing multiple copies of a ligand provide an effective strategy for inhibiting multimeric receptors.^[7,8] For example, multivalent derivatives of GM1,^[9,10] or related oligosaccharides,^[11–15] are potent inhibitors of B-pentamer adhesion to GM1-coated surfaces; an octavalent GM1-dendrimer has been shown to be 47 500 times more efficient as an inhibitor than an equivalent concentration of monovalent GM1.^[10] Multivalent lectins with binding sites arranged on opposing faces of the protein, for example, galectins,^[16,17] concanavalin A^[18] or soybean agglutinin,^[19] generally form cross-linked aggregates with both their natural ligands and synthetic multivalent inhibitors. In contrast, theoretical models describing multivalent interactions of cholera toxin usually assume that the protein does not aggregate as the binding sites are all on the same face of the multimeric protein;^[20,21] however, ligand-induced dimerization of pen-

tameric receptors has been observed in crystal structures.^[8,22,23] Here we demonstrate that multivalent GM1-inhibitors with mismatched valencies can operate through protein aggregation. Furthermore, we show that the valency of the inhibitor

[a] A. J. Baron, Dr. S. D. Connell, E. D. Hayes, Dr. W. B. Turnbull
Astbury Centre for Structural Molecular Biology, University of Leeds
Leeds, LS2 9JT, (UK)

[b] C. Sisu, E. D. Hayes, Dr. W. B. Turnbull
School of Chemistry, University of Leeds
Leeds, LS2 9JT (UK)
Fax: (+44) 113-343-6565
E-mail: w.b.turnbull@leeds.ac.uk

[c] Dr. S. D. Connell
School of Physics and Astronomy, University of Leeds
Leeds, LS2 9JT (UK)

[d] C. Sisu, Dr. C. A. G. M. Weijers, A. V. Pukin, Prof. Dr. H. Zuilhof,
Dr. G. M. Visser
Laboratory of Organic Chemistry, Wageningen University
Dreijenplein 8, 6703 HB Wageningen (The Netherlands)
Fax: (+31) 317-484-914
E-mail: han.zuilhof@wur.nl

[e] Dr. R. de Vries
Laboratory of Physical Chemistry and Colloid Science
Wageningen University
P.O. Box 8038, 6700 EK Wageningen (The Netherlands)

[f] Dr. H. M. Branderhorst, Dr. R. J. Pieters
Department of Medicinal Chemistry and Chemical Biology
Utrecht Institute for Pharmaceutical Sciences, Utrecht University
P.O. Box 80082, 3508 TB Utrecht (The Netherlands)

[g] Dr. M. Gilbert
Institute for Biological Sciences, National Research Council of Canada
100 Sussex Drive, Ottawa, Ontario K1A 0R6 (Canada)

Supporting information for this article is available on the WWW under <http://www.chembiochem.org> or from the author.

has a dramatic effect on the mechanism of aggregation, influencing both the kinetics of aggregation and the stability of intermediate protein complexes.

Results and Discussion

The divalent and tetravalent GM1 analogues **GM1-2** and **GM1-4** (Figure 1) have been shown to inhibit cholera toxin B-pentamer (CTB) binding in an ELISA experiment (Table 1).^[10] IC₅₀

values were found to be four to five orders of magnitude lower than those for monovalent GM1 derivative **GM1-1**.^[24] In the present study we found that these compounds are also active against the B-pentamer of *E. coli* heat-labile toxin (LTBh) which has identical GM1 binding sites to CTB.^[25] Although there are subtle differences in the binding affinities of CTB and LTB isoforms for a range of ligands,^[26] CTB and LTB are often used interchangeably when testing inhibitors. While our previous experiments involved direct detection of a CTB-horseradish

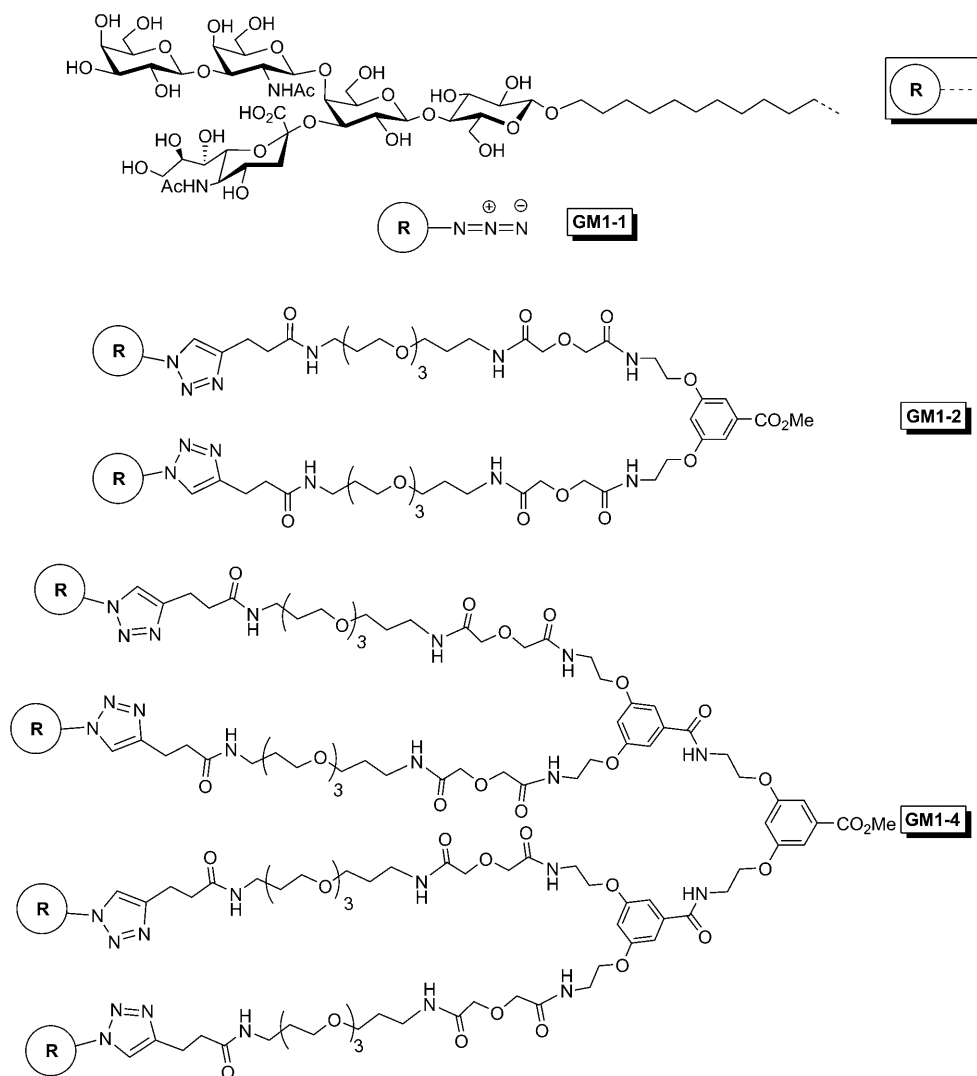


Figure 1. Structures of the ganglioside GM1 mimics bearing one, two and four oligosaccharide ligand groups.

Table 1. Comparison of CTB and LTBh inhibition in ELISA assays. ^[a]								
Ligand	IC ₅₀ [nM] ^[b]		Hill coefficient		B-subunit concentration [nM] ^[e]		GM1-groups per B-subunit at IC ₅₀ ^[f]	
	CTB ^[c]	LTBh	CTB	LTBh	CTB	LTBh	CTB	LTBh
GM1-1	19 000 ± 6 000	> 200 000	0.5	0.5 ^[d]	2.1	19	9 047	> 10 500
GM1-2	2.0 ± 1.0	21 ± 7	1.0	0.7	2.1	19	1.9	2.1
GM1-4	0.23 ± 0.07	31 ± 3	3.0	3.0	2.1	19	0.4	6.3

[a] All experiments employed microtitre plates coated with 0.2 µg GM1 per well and blocked with BSA. [b] Concentration of the multivalent ligand for 50% inhibition of toxin binding (not normalized for ligand valency). [c] CTB data is taken from reference [10] [d] This value was chosen for the curve fitting based on the CTB result. [e] Concentration of binding sites (i.e. 5 × the B-pentamer concentration). [f] Ligand valency × IC₅₀/[B-subunit].

peroxidase conjugate,^[10] here the LTBh pentamer was detected using a traditional indirect ELISA assay. The lower sensitivity of the LTBh ELISA assay made it necessary to use a ten-fold higher B-pentamer concentration than that employed previously. Therefore the IC₅₀ values for LTBh are higher than those measured for CTB (Figure 2; Table 1). Inhibitors **GM1-2** and

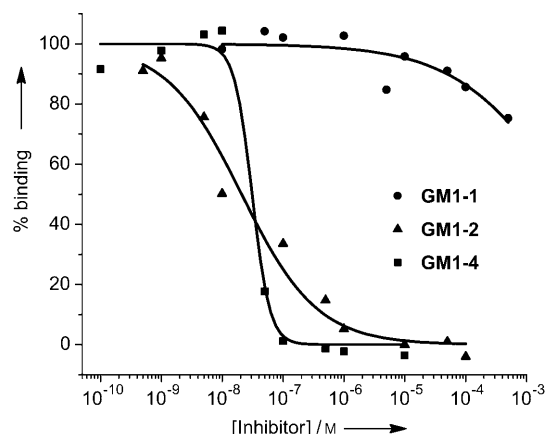


Figure 2. ELISA assay showing inhibition of LTBh (3.8 nM pentamer concentration) binding to a GM1-coated microtitre plate.

GM1-4 were found to have IC₅₀ values of 20–30 nM, while the monovalent GM1 derivative **GM1-1** showed only 25% inhibition at 100 μM. Although the absolute values differ from the CTB experiments, the *relative* inhibitory potencies of the multivalent and monovalent ligands are similar for the two proteins; inhibition of LTBh binding to GM1 displayed at a surface is greatly enhanced through multivalency.

Isothermal titration calorimetry (ITC) was used to measure the affinity of the ligands for LTBh. In all experiments the ligand was added to a solution of the protein and binding stoichiometries were calculated in terms of the number of oligosaccharide groups per binding site (see the Supporting Information for example titration curves and discussion of curve fitting at high *c* values). ITC experiments (Table 2) revealed that monovalent **GM1-1** bound to LTBh has a *K_d* slightly lower than that reported previously for the CTB-GM1 oligosaccharide interaction (43 nM).^[27] However, **GM1-2** and **GM1-4** showed less than a five-fold increase in affinity and only a small change in the enthalpies of interaction compared to equivalent concentrations of the monovalent ligand **GM1-1**. The expected 1:1 binding stoichiometry (i.e., one GM1 oligosaccharide binding

per LTBh subunit) was observed in all cases; this demonstrates that all protein binding sites are accessible to the ligands.^[28]

The presence of the multivalent scaffold appears neither to enhance nor perturb the individual interactions between the protein and oligosaccharide. This result demonstrates that the increased potency observed for the multivalent inhibitors in the ELISA assay^[10] can not be attributed to a change in the intrinsic affinity of the oligosaccharide for the protein. Since it was noted that the solutions became hazy during the titrations, the question arose whether the activity of the multivalent ligands could result from protein aggregation. Such a mechanism can not be deduced from the ITC data, because ITC only describes the extent of receptor saturation as a function of ligand concentration—it does not reveal to what extent the multivalent ligands crosslink subunits within a pentameric receptor rather than crosslink subunits in different pentamers.

Sedimentation velocity analytical ultracentrifugation (SV-AUC)^[29,30] was used to detect the extent of protein oligomerisation in the presence of various concentrations of the inhibitors. Figure 3A shows that the pure LTBh solution contained a single species with a sedimentation coefficient of 4.4 ± 0.1 S; this corresponds to the expected mass of 58 kDa for the LTBh pentamer. Addition of divalent inhibitor **GM1-2** to give total GM1 concentrations of 0.1 and 0.2 equivalents per LTBh binding site led to a new species at 7.8 ± 0.2 S with a predicted mass of approximately 125 kDa; i.e., a dimeric complex of the LTBh pentamer. A dramatic reduction in signal was observed upon increasing the concentration of inhibitor **GM1-2** to 0.5 equivalents of GM1 groups per LTBh binding site. At or below this concentration, the majority of the protein formed rapidly sedimenting aggregates of high mass that were beyond the limits of the optical detection system and could not be observed under the conditions of the SV-AUC experiment. Further addition of inhibitor **GM1-2** up to one equivalent of GM1 groups resulted in almost complete dimerization of the fraction of LTBh protein that remained visible to the AUC optics. In contrast, the same concentration of monovalent **GM1-1** did not significantly change the sedimentation coefficient of the protein (Figure 3A).

The tetravalent inhibitor **GM1-4** showed a more gradual reduction in signal intensity above 0.2 equivalents of GM1 groups per LTBh binding site (Figure 3B), and there was no evidence for LTBh dimerization.

Dynamic light scattering experiments were performed on LTBh in the presence and absence of **GM1-2** and **GM1-4** to further characterize the formation of the aggregates. The field au-

Table 2. Thermodynamics of GM1 derivatives binding to LTBh.^[a]

Ligand	<i>K_d</i> [nM]	Δ <i>G</i> [°] [kcal mol ^{−1}]	Δ <i>H</i> [°] [kcal mol ^{−1}]	<i>T</i> Δ <i>S</i> [°] [kcal mol ^{−1}]	<i>n</i>
GM1-1	9.0 ± 0.9 ^[b]	−10.97 ± 0.06	−20.30 ± 0.19	−9.33 ± 0.11	0.99 ± 0.01
GM1-2	3.6 ± 0.2	−11.50 ± 0.03	−21.32 ± 0.43	−9.82 ± 0.20	1.00 ± 0.04
GM1-4	6.9 ± 2.0	−11.15 ± 0.15	−20.95 ± 0.31	−9.80 ± 0.22	1.00 ± 0.01

[a] The GM1 derivative was titrated into a solution of LTBh (4–10 μM subunit concentration) at 298 K to give a final GM1:LTBh subunit ratio of approximately 2:1. [b] Errors in *K_d*, Δ*H*[°] and *n* are the standard deviation of multiple experiments. Errors in Δ*G*[°] and *T*Δ*S*[°] were determined using Monte Carlo simulations (see the Experimental Section).

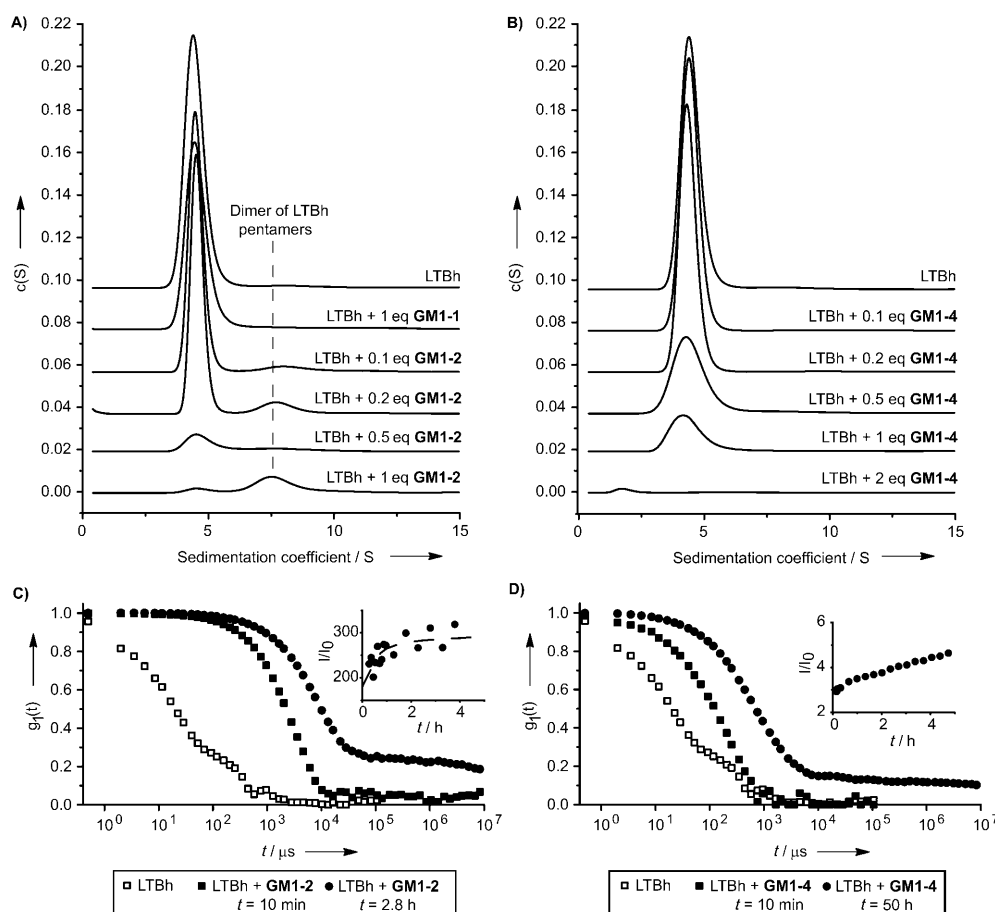


Figure 3. Sedimentation coefficient distributions $[c(s)]$ for mixtures of LTBh (2 μM pentamer concentration, 10 μM GM1 binding sites) with varying concentrations of A) GM1-1 and GM1-2, and B) GM1-4; the number of equivalents of ligand is expressed as the number of GM1 oligosaccharide groups per LTBh binding site. Dynamic light scattering field autocorrelation functions $[g_2(t)]$ for LTBh alone (1.4 μM pentamer concentration) and in the presence of either C) GM1-2 or D) GM1-4 (0.1 equiv GM1 groups per LTBh binding site) are shown at various times after mixing. The scattering intensity, I for each ligand normalized by the scattering of LTBh protein alone (I_0) is shown as a function of time after mixing in the inset graphs in parts C) and D).

to correlation function for LTBh corresponded to a dominant species with a hydrodynamic radius of 4.0 ± 0.1 nm (Figure 3C and D). On addition of GM1-2 to give 0.1 equivalents of GM1 groups per LTBh binding site, the scattered intensity increased dramatically (Figure 3C inset), reaching a maximum scattering intensity approximately one hour after mixing. The analogous concentration of GM1-4 led to a more modest increase in the light scattering (Figure 3D inset). The field autocorrelation functions for the aggregates also developed over time, and again the changes in the GM1-2 curves were much more rapid than those for GM1-4 (Figure 3C and D). For GM1-2, the average hydrodynamic radius of the aggregates was 1.1 ± 0.2 μm during the first five hours of the aggregation process, whereas in the case of GM1-4 the initial aggregates with radii of approximately 50 nm grew to a few hundred nm over two days. In both cases, the aggregation process led to field autocorrelation functions that no longer decayed to zero. This is indicative of the formation of a space-filling network in which the positions of some of the particles are effectively fixed such that there are residual positional correlations, even at very long

times. Small amounts of large aggregates dominate the DLS signal, and the DLS data do not contradict that a majority (>95%) of LTBh still exists as pentamers or dimers of pentamers as indicated by AUC. Nevertheless, it is remarkable that such a network already forms when only one binding site in ten is occupied by ligand. Control experiments with analogous non-binding multivalent ligands demonstrated that protein aggregation was dependent on specific GM1–LTBh interactions and was not a result of nonspecific interactions with the dendritic scaffolds or “salting-out” mechanisms associated with the phosphate buffer (see the Supporting Information).

After about 10 h the scattering intensity of the LTBh/GM1-2 mixture started to decrease and ultimately reached a level only a few times higher than that for LTBh alone. A similar observation was made for an LTBh/GM1-4 mixture comprising 0.5 GM1 groups per binding site. The most plausible reason is that the fragile network was slowly sedimenting under the force of gravity. This result is in accord with the observation that the solutions became hazy during the

ITC experiments, but did not precipitate. Precipitation would have led to a discontinuity in the baseline resulting from a change in the capacity of the system; as no such discontinuity was observed, the aggregates remained in solution. In contrast, the high centrifugal forces used in the AUC experiments would cause the aggregates to sediment as soon as they were formed. Therefore, the extent of LTBh precipitation during the AUC experiments may reflect the rate of aggregation rather than the stability of the aggregates as such.

Our results are in stark contrast to those reported by Merritt et al.^[12] and Pickens et al.^[13] who also used DLS experiments to study pentavalent inhibitors for LTB and divalent inhibitors for CTB, respectively. In each case the authors observed no evidence for protein aggregation, even when working at CTB or LTB concentrations five- to ten-times higher than those employed in the present study. Dimerization of CTB has only been observed using a decavalent ligand, and no higher aggregates were formed.^[23]

As the divalent GM1-2 and tetravalent GM1-4 gave essentially identical ITC binding parameters and differ only marginal-

ly in the distance between the oligosaccharide head groups, their contrasting solution behavior must be attributed to their different valencies. The ligands were designed such that the long flexible linkers would be able to bridge adjacent binding sites within an LTBh pentamer. However, **GM1-2** gives rise to a significant amount of dimerization of LTBh pentamers throughout the titration (Figure 3A). Upon cross-linking two independent particles in solution, a significant entropic penalty must be paid for loss of independent translational and rotational degrees of freedom.^[27,31] Therefore, intrapentamer binding would be expected to predominate. However, the entropic advantage of chelation must be balanced against the loss of conformational entropy that occurs when a flexible ligand binds two binding sites within an LTBh pentamer.^[31] At low ligand concentrations, most dimers of LTBh pentamers are connected by a single **GM1-2** molecule. It is likely that the long flexible linker in **GM1-2** allows substantial independent motion of the LTBh pentamers within the ternary complex, which should reduce the entropic penalty expected for protein dimerization (Figure 4A). For the dimeric ligand **GM1-2**, the maximisation of conformational entropy within the complex appears to be more favourable than maximising the number of independent particles in the system.

The tetravalent inhibitor **GM1-4** could also form complexes in which it bridges two LTBh pentamers (Figure 4B); however, none are observed in the AUC experiment (Figure 1B). Any ternary complex in which all GM1 groups are bound would involve crosslinking of the **GM1-4** ligand with adjacent LTBh subunits and concomitant rigidification of the dendritic linker (Figure 4B). None of these configurations would have the same level of residual conformational entropy that would be observed for the ternary complex in Figure 4A. One might therefore assume that the 1:1 **GM1-4**/LTBh pentamer complex would predominate until 80% of the LTBh binding sites were filled. However, the DLS experiments show that aggregation already occurs when only 10% of the binding sites are filled. Therefore, the 1:1 complex is not the only species present in solution, and unlike **GM1-2**, crosslinking occurs without significant accumulation of dimers of LTBh pentamers. Indeed, as intra-pentamer binding is disfavoured for the **GM1-2** ligand, a ternary complex in which two LTBh pentamers are linked by only two ligand groups of **GM1-4** (Figure 4C) would be preorganised to aggregate with the pentamers in a face-to-face orientation. A similar aggregate could form with the divalent **GM1-2** ligand once two to three binding sites per LTBh pentamer are occupied (Figure 4D). This observation would account for the dramatic increase in aggregation that was observed in the AUC experiment (Figure 3A) for 0.5 equivalents of GM1 groups per LTBh binding site.

In the case of **GM1-2** it is notable that dimers of LTBh pentamers continue to exist at equimolar concentrations of GM1 ligand groups and LTBh binding sites (Figure 3A). The ITC experiments indicate that essentially all ligand is bound to the protein around the equivalence point of the titration. There are three possible configurations for a 2:5 LTBh pentamer:**GM1-2** complex (Figure 4E) in which the valencies of the ligand and receptors are matched such that the complexes are

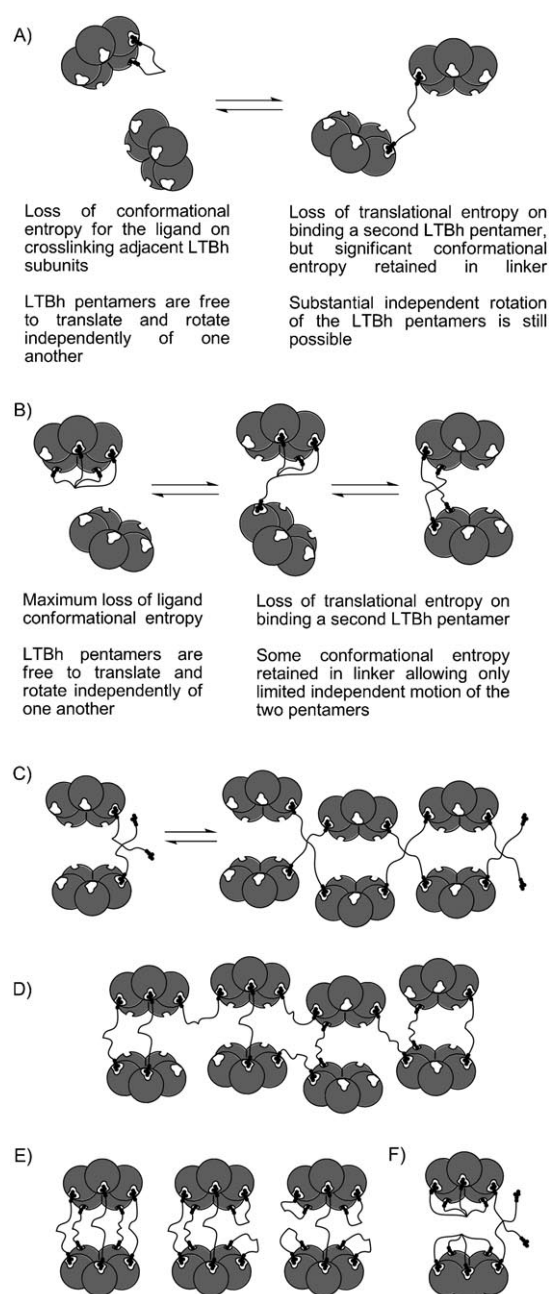


Figure 4. Schematic representation of LTBh dimerization at A) low concentrations of divalent **GM1-2** and B) low concentrations of tetravalent **GM1-4**. Examples of face-to-face aggregates that could form at sub-stoichiometric concentrations of C) **GM1-4**, and D) **GM1-2**. E) Three possible configurations for a 2:5 LTBh pentamer:**GM1-2** complex in which all binding sites are occupied. F) An example of a 2:3 LTBh pentamer:**GM1-4** complex illustrating the mismatched valencies between the ligands and receptors.

unable to make further interactions with either **GM1-2** or LTBh. A similar complex that is saturated with tetravalent **GM1-4** ligands would require a stoichiometry of 2:3 LTBh pentamer:**GM1-4**. There are many possible configurations for such a complex (one example is shown in Figure 4F), but in all cases the valencies of ligands and receptors are mismatched. If all GM1 ligand groups are to become bound to LTBh, then aggre-

gation must occur. In contrast, the pentavalent ligands reported by Fan, Hol and co-workers have valencies that match the LTB/CTB proteins precisely and only 1:1 complexes are observed,^[12] even at protein concentrations five to ten times higher than those used in the present study.

We thus presume that the matched valencies (2:5 LTBh pentamer:GM1-2) allow the dimer of LTBh pentamers to persist toward the end of the titration. Whitesides and co-workers recently described the formation of bicyclic trimers of divalent antibodies and trivalent dinitrophenyl ligands.^[32] High molecular weight aggregates form initially on mixing the components, but rearrange to form only discrete complexes at equilibrium, of which the 3:2 IgG:ligand complex predominates at the appropriate stoichiometric ratio. In our AUC experiments, the formation of large aggregates is probably also under kinetic control, but the persistence of the dimers of LTBh pentamers suggests that they are thermodynamically stable under the conditions of the experiment. Indeed, a novel strategy for inhibiting bacterial toxins through the formation of defined seven-component aggregates has been reported independently by both Fan^[33] and Bundle.^[34] A pentavalent pentraxin protein and either CTB^[33] or shiga toxin B-pentamer^[34] are brought together to form stable heterodimers that are crosslinked by five copies of a heterobifunctional ligand. In both cases the overall stability of the complex was substantially greater than the individual monovalent interactions.

The aggregation mechanisms proposed here for ligands GM1-2 and GM1-4 both assume that aggregation would involve crosslinking the LTBh pentamers in which the binding face of one pentamer is brought into close proximity with the binding face of additional pentamers (Figure 4C and D). Atomic force microscopy (AFM) has been used previously to study CTB adhered to mica and lipid bilayers under aqueous conditions.^[35,36] Figure 5A shows the LTBh pentamers as round particles distributed across a mica surface. At higher resolution (Figure 5B) it is possible to resolve individual subunits and a depression at the centre of the particles that corresponds to the central pore. The 6.5 nm width and 3.5 nm height of these particles (Figure 5E) is in good agreement with the dimensions of the pentamer determined from the crystal structure of the porcine variant of the protein LTBp (Figure 5F).^[37] In the presence of two equivalents of the divalent GM1-2 ligand, the protein appears as aggregates of irregular diameter, but a remarkably consistent height of 6.5 nm. The increased height of the aggregates is consistent with a head-to-head dimerization that either prevents the LTBh pentamer from sitting flat on the surface, or gives rise to a protein bilayer. Surprisingly, LTBh bound to monovalent ligand GM1-1 also forms aggregates (Figure 5D), although individual particles can also still be seen (indicated by white arrows, Figure 5D). In this case the aggregates have an average height of 3.5 nm which excludes the possibility that LTBh dimers form in the presence of the monovalent ligand GM1-1.

The function of many multivalent lectins depend on aggregating their carbohydrate ligands.^[16,38,39] The aggregation processes observed in this study occur at physiologically relevant concentrations of the protein toxin. Turnbull et al.,^[5] have de-

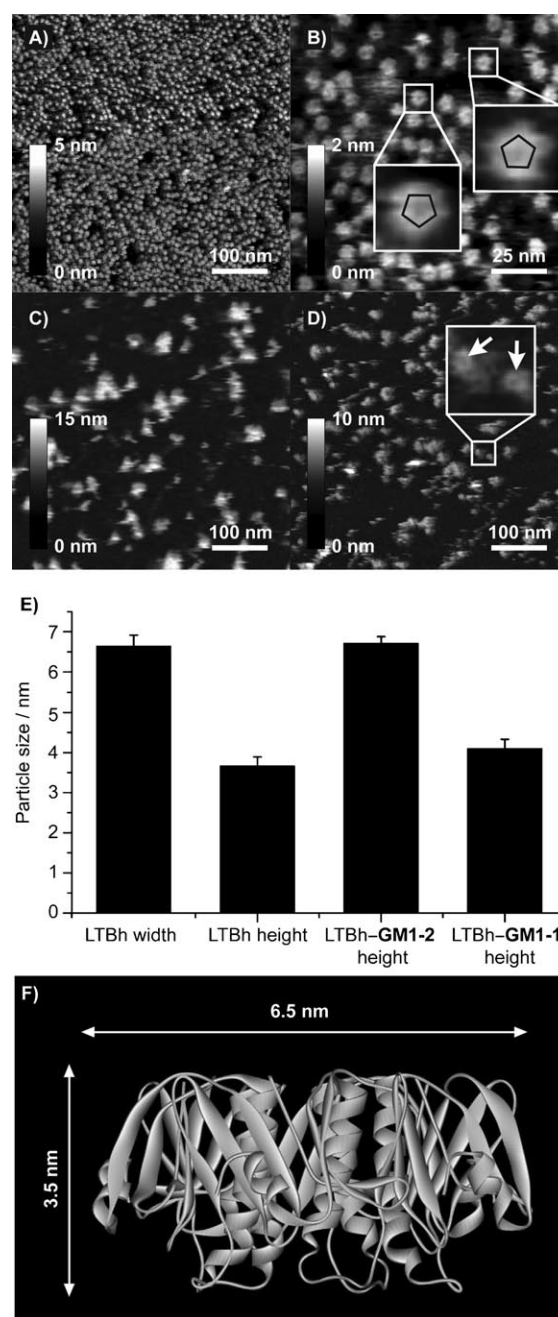


Figure 5. Atomic force microscopy images of pure LTBh (ca. 67 nM pentamer concentration) show A) uniform round particles adhered to the mica surface. B) Individual subunits can be seen at higher resolution. C) In the presence of divalent inhibitor GM1-2 the protein forms aggregates. D) The monovalent inhibitor GM1-1 also aggregates the protein but individual pentamers are still visible (inset). E) The average heights and widths of LTBh pentamers and their aggregates are in accord with F) the dimensions of the protein determined crystallographically.

tected 10 $\mu\text{g mL}^{-1}$ cholera toxin in human rice-water stool samples (conditions under which aggregates were observed by AFM). Moreover, these authors note that the concentration of the toxin in vivo is a balance of the rates of its production and excretion in diarrhoeal fluid. Inhibitors such as GM1-2 and GM1-4 are designed to prevent the toxin from entering endothelial cells and thus avoid the downstream biochemical

events that would lead to diarrhea. However, these inhibitors are not expected to reduce the rate of toxin production. Therefore, during a course of anti-adhesion therapy, the concentration of the toxins would likely increase further.

At these micromolar concentrations, the enhanced activity of the compounds arises principally from aggregation of the protein receptors to form space-filling networks, even at sub-stoichiometric ligand:receptor ratios. While it is generally accepted that multivalency is an effective strategy for increasing the activity of inhibitors, we have demonstrated that the valency of the inhibitor can also have a substantial effect on both the kinetics and mechanism of aggregation. Ligand valency determines if discrete multicomponent complexes can form; stable dimers of the LTBh pentamers arise only if the valencies of the ligand and receptor can be matched. No aggregation was observed in previous studies of pentavalent inhibitors when using higher B-pentamer concentrations than those employed here.^[12,13] Thus, it would appear that discrete complexes will arise when the valencies of ligand and receptor are matched, but aggregates will form when the valencies are mismatched. This observation is central to the design of well defined multi-component biomolecular assemblies.^[32] When one considers that tetravalent galactosyl dendrimers^[10] have been shown to be more potent inhibitors than pentavalent galactosyl ligands of similar size,^[40] it is also tempting to conclude that mismatched valencies may provide a more effective general strategy for the development of multivalent therapeutics against bacterial toxins. Of course, these tetravalent and pentavalent compounds differ in the exact structure of their flexible arms, and so it would be necessary to make pentavalent ligands analogous to **GM1-4** for an accurate comparison of inhibitory activities. Although aggregation occurs at physiologically relevant low μM concentrations, it is not clear if the ligands operate by the same aggregative mechanism at nanomolar concentrations at which these compounds were found to be effective inhibitors in ELISA assays.^[10] New, more sensitive biophysical methods will be required to study these aggregation phenomena at nanomolar concentrations and below. A deeper understanding of the mechanisms of multivalent interactions will lead to more effective inhibitors against multimeric proteins and further enable the rational design of supramolecular assemblies for bionanoscience.^[32,41–43]

Experimental Section

Sample preparation: Compounds **GM1-1**, **GM1-2** and **GM1-4** were prepared as reported previously.^[10,24] Buffers and other reagents were bought from Sigma or Fisher unless stated otherwise.

A *Vibrio sp.60* clone harbouring the pMMB68 plasmid encoding LTBh originally reported by Amin and Hirst^[44] was kindly provided by B. L. Precious, University of St Andrews. Bacterial cultures were grown at 37 °C in Luria–Bertani NaCl enriched medium (1 % tryptone, 0.5 % yeast extract and 2 % NaCl) in the presence of carbenicillin (100 $\mu\text{g mL}^{-1}$). Upon reaching $\text{OD}_{600} = 0.40$, protein production was induced by addition of isopropyl- β -thiogalactoside (1 mM final concentration), and the cultures were grown for a further 24 h at 37 °C. Cells were pelleted by centrifugation and the LTBh protein

was precipitated from the supernatant by addition of either ammonium sulfate (60 % saturation), or sodium hexametaphosphate (2.5 g L^{-1}) and adjusting the pH to 4.5. The precipitate was collected by centrifugation and re-suspended in sodium phosphate buffer (50 mL, 0.1 M, pH 8.0), before dialysis against sodium phosphate (10 mM, pH 7.4). After removing insoluble material by centrifugation, the protein preparation was passed over a Ni^{2+} -NTA column that had been pre-equilibrated with 10 bed volumes of dialysis buffer. The column was washed (10 bed volumes, 50 mM Tris-HCl, 500 mM NaCl, 10 mM imidazole, pH 7.4), and eluted with elution buffer (20 mL, 50 mM Tris-HCl, 500 mM NaCl, 250 mM imidazole, pH 7.4). The collected fractions were dialysed against sodium phosphate buffer (20 mM phosphate, 100 mM NaCl, pH 7.4) for storage at 4 °C. The protein purity was determined by SDS-PAGE analysis and its concentration was evaluated by UV absorption at 280 nm using a theoretical molar extinction coefficient of 11 585 $\text{M}^{-1} \text{cm}^{-1}$.

Enzyme-linked immunosorbent assay: LTBh inhibition assays were carried out using the following solutions and buffers: phosphate-buffered saline (PBS) buffer, blocking buffer (1 % bovine serum albumin (BSA) in PBS), washing buffer (0.1 % BSA, 0.05 % Tween-20 in PBS), primary antibody VD12 (mouse-anti LTBh)^[45] and secondary antibody (sheep-anti-mouse alkaline phosphatase labelled). The alkaline phosphatase substrate solution comprised of 4-nitrophenyl phosphate disodium hexahydrate (7.5 mg) dissolved in Tris buffer (10 mL, 0.1 M Tris, 5 mM MgCl_2 , pH 9.6).

A 96-well plate was coated with a solution of GM1 (100 μL , 2 $\mu\text{g mL}^{-1}$) in PBS buffer. Unattached ganglioside was removed by washing with PBS and the remaining binding sites of the surface were blocked with BSA (1 %) in PBS, and finally washed with PBS. Samples of LTBh (3.8 nM pentamer concentration) and inhibitor (0.1–100 000 nM) in washing buffer were incubated at RT for 2 h before adding to the GM1-coated plate. After 1 h of incubation at room temperature the solution was removed and the wells were washed with washing buffer. Primary antibody VD12 (100 μL in blocking buffer) was added to the wells. After 1 h of incubation at room temperature, the solution was removed and the wells were washed with washing buffer. The secondary antibody solution (100 μL) was added to the wells and incubated for 45 min at room temperature. Excess antibody solution was then removed and the wells were washed with washing buffer. To identify antibody labelled-toxin binding to surface-bound GM1 the wells were treated with alkaline phosphatase substrate solution (150 μL). The absorbance of each well was recorded at 415 nm every 15 min for a total incubation interval of 45 min.

Isothermal titration calorimetry: ITC experiments were performed using a VP-ITC calorimeter (Microcal Inc. Northampton, MA, USA), with a cell volume of 1.409 mL. All titrations were conducted at 25 °C in sodium phosphate (20 mM, pH 7.4) containing NaCl (100 mM). The LTBh protein was dialysed against this buffer three times before diluting the protein to a final LTB-subunit concentration of 4–10 μM . GM1-derivatives were dissolved in the buffer from the final dialysis step. Protein and ligand concentrations were determined by UV absorption. The GM1 derivatives were added to the LTBh solution in titrations typically comprising 24 injections (8 μL) at 4 min intervals. Separate titrations of ligands into the same buffer were used to subtract the heat of dilution from the integrated data prior to curve fitting using the built-in one site model. Errors were propagated using Monte Carlo simulations in Microsoft Excel or Origin.^[46] Typically 1000–5000 ΔH° and K_d values were simulated by adding random error to the mean values of these parameters determined from multiple ITC experiments. The

added error had a Gaussian distribution with a mean of zero and a standard deviation equal to the standard deviation for each experimentally derived parameter (K_a and ΔH°). The simulated ΔH° and K_a values were used to calculate 1000–5000 values for ΔG° and $T\Delta S^\circ$, the mean and standard deviations of which are reported in Table 2.

Analytical ultracentrifugation: The partial molar volume of LTBh, buffer densities and viscosities were calculated using SEDNTERP (<http://www.jphilo.mailway.com/download.htm>). The partial molar volumes for the **GM1-2** and **GM1-4** were predicted using the protocol outlined in ref. [47]. However, control experiments conducted in the absence of protein failed to give an adequate UV absorbance at 280 nm to allow accurate curve fitting, even at the highest concentration used (20 μM oligosaccharide concentration). Protein and ligand samples were prepared as in the ITC experiments. Mixtures of toxin with various amounts of ligands were prepared immediately before analysis. The samples (0.42 mL) were centrifuged in 1.2 cm pathlength 2-sector aluminium centrepiece cells (sample in RH sector, reference buffer in LH sector) with sapphire windows in an 8-place An-50 Ti analytical rotor running in an Optima XL-I analytical ultracentrifuge (Beckman Instruments Inc., Fullerton, CA, USA) at 35 000 rpm and at a temperature of 20.0 $^\circ\text{C}$. Changes in solute concentration were detected by Rayleigh interference and 280 nm radial absorbance. 102 scans of each type were collected from each cell during 16 h. Results were analysed by whole-boundary profile analysis using the program Sedfit v 11.3 (P. Schuck, NIH).^[48]

Dynamic Light scattering: DLS was performed using a Malvern NanoS, operating at a scattering angle of 173 $^\circ$, using a HeNe laser with a wavelength $\lambda = 633$ nm. All measurements were performed at a temperature of 25 $^\circ\text{C}$. Effective hydrodynamic radii reported are based on either a monomodal or a bimodal distribution fit of the field autocorrelation function $g_1(t)$, as reported by the Malvern DTS software, version 5.00 (Malvern, UK). Absolute scattering intensities were determined by using toluene as a reference, with an absolute value for the toluene scattering of $R_{\text{toluene}} = 0.0013522 \text{ m}^{-1}$. The LTBh, **GM1-2** and **GM1-4** stock solutions and buffer were filtered using 100 kDa cut-off Amicon centrifuge filters (Billerica, MA, USA). A 10% reduction of the concentration of the LTBh stock solution due to filtration was taken into account in determining final protein concentrations. Samples for scattering were prepared by mixing the filtered components in a carefully cleaned quartz cuvette in a laminar flow hood.

Atomic force microscopy: It has been shown previously that CTB will spontaneously adhere to a mica surface under aqueous conditions.^[35,36] However, LTBh proved to interact very weakly with mica at neutral pH, presumably because the protein is close to its isoelectric point at that pH. Therefore, all AFM experiments were conducted in a citrate-phosphate buffer at pH 6. A solution of LTBh (0.2 μM pentamer concentration), in citrate-phosphate buffer (2 mM sodium phosphate, 2 mM sodium citrate, 10 mM NaCl, pH 6.0) was incubated on a freshly cleaved mica disk for 10 mins before diluting three-fold with the same buffer. AFM height images were recorded under buffer using a Nanoscope IIIa Multi-mode AFM (Digital Instruments, Veeco Metrology Group, Inc., Santa Barbara, CA, USA) and silicon nitride cantilevers (NP-S, Veeco Metrology Group). The cantilevers had a spring constant of approximately 0.32 N m^{-1} . The height images reported here are raw, unfiltered data, line levelled using a simple polynomial fit, and obtained by tapping (dynamic) mode at a frequency in the range of 25–27 kHz with a 95% set-point. Accurate width measurements of subunits were obtained by measuring the periodicity within close-

packed clumps, thereby negating the effect of tip-magnification of small objects due to tip-sample convolution.

Acknowledgements

This work was supported by funding from the Royal Society, NanoNed, the Graduate School VLAG (Wageningen, The Netherlands) and the Utrecht Institute for Pharmaceutical Sciences (UIPS). We thank the EU for fostering collaboration in this area: EU COST working group D34/0001/05 "Multivalent ligands for cholera toxin inhibition and sensing". W.B.T. is the recipient of a Royal Society University Research Fellowship. E.D.H. is supported by a BBSRC CASE award in collaboration with AstraZeneca. We thank the Wellcome Trust for supporting the Astbury Centre AUC facility through a JIF award.

Keywords: aggregation • carbohydrates • cholera • dendrimers • multivalency

- [1] D. A. Sack, R. B. Sack, G. B. Nair, A. K. Siddique, *Lancet* **2004**, 363, 223–233.
- [2] S. S. Al-Abri, N. J. Beeching, F. J. Nye, *Lancet Infect. Dis.* **2005**, 5, 349–360.
- [3] E. A. Merritt, W. G. Hol, *Curr. Opin. Struct. Biol.* **1995**, 5, 165–171.
- [4] D. Vanden Broeck, C. Horvath, M. J. S. De Wolf, *Int. J. Biochem. Cell Biol.* **2007**, 39, 1771–1775.
- [5] P. C. Turnbull, J. V. Lee, M. D. Miliotis, C. S. Still, M. Isaacson, Q. S. Ahmad, *J. Clin. Microbiol.* **1985**, 21, 884–890.
- [6] I. A. Velter, M. Politi, C. Podlipnik, F. Nicotra, *Mini-Rev. Med. Chem.* **2007**, 7, 159–170.
- [7] M. Mammen, S.-K. Chio, G. M. Whitesides, *Angew. Chem.* **1998**, 110, 2908–2953; *Angew. Chem. Int. Ed.* **1998**, 37, 2754–2794.
- [8] P. I. Kitov, J. M. Sadowska, G. Mulvey, G. D. Armstrong, H. Ling, N. S. Pannu, R. J. Read, D. R. Bundle, *Nature* **2000**, 403, 669–672.
- [9] J. P. Thompson, C.-L. Schengrund, *Biochem. Pharmacol.* **1998**, 56, 591–597.
- [10] A. V. Pukin, H. M. Branderhorst, C. Sis, C. A. G. M. Weijers, M. Gilbert, R. M. J. Liskamp, G. M. Visser, H. Zuilhof, R. J. Pieters, *ChemBioChem* **2007**, 8, 1500–1503.
- [11] H. M. Branderhorst, R. M. J. Liskamp, G. M. Visser, R. J. Pieters, *Chem. Commun.* **2007**, 5043–5045.
- [12] E. A. Merritt, Z. Zhang, J. C. Pickens, M. Ahn, W. G. J. Hol, E. Fan, *J. Am. Chem. Soc.* **2002**, 124, 8818–8824.
- [13] J. C. Pickens, D. D. Mitchell, J. Liu, X. Tan, Z. Zhang, C. L. M. J. Verlinde, W. G. J. Hol, E. Fan, *Chem. Biol.* **2004**, 11, 1205–1215.
- [14] D. Arosio, M. Fontanella, L. Baldini, L. Mauri, A. Bernardi, A. Casnati, F. Sansone, R. Ungaro, *J. Am. Chem. Soc.* **2005**, 127, 3660–3661.
- [15] D. Arosio, I. Vrasidas, P. Valentini, R. M. J. Liskamp, R. J. Pieters, A. Bernardi, *Org. Biomol. Chem.* **2004**, 2, 2113–2124.
- [16] C. F. Brewer, M. C. Miceli, L. G. Baum, *Curr. Opin. Struct. Biol.* **2002**, 12, 616–623.
- [17] G. A. Rabinovich, M. A. Toscano, S. S. Jackson, G. R. Vasta, *Curr. Opin. Struct. Biol.* **2007**, 17, 513–520.
- [18] S. M. Dimick, S. C. Powell, S. A. McMahon, D. N. Moothoo, J. H. Naismith, E. J. Toone, *J. Am. Chem. Soc.* **1999**, 121, 10286–10296.
- [19] J. C. Sacchettini, L. G. Baum, C. F. Brewer, *Biochemistry* **2001**, 40, 3009–3015.
- [20] J. M. Gargano, T. Ngo, J. Y. Kim, D. W. K. Acheson, W. J. Lees, *J. Am. Chem. Soc.* **2001**, 123, 12909–12910.
- [21] P. I. Kitov, D. R. Bundle, *J. Am. Chem. Soc.* **2003**, 125, 16271–16284.
- [22] M. B. Pepys, J. Herbert, W. L. Hutchinson, G. A. Tennent, H. J. Lachmann, J. R. Gallimore, L. B. Lovat, T. Bartfai, A. Alanine, C. Hertel, T. Hoffmann, R. Jakob-Roetne, R. D. Norcross, J. A. Kemp, K. Yamamura, M. Suzuki, G. W. Taylor, S. Murray, D. Thompson, A. Purvis, S. Kolstoe, S. P. Wood, P. N. Hawkins, *Nature* **2002**, 417, 254–259.

- [23] Z. Zhang, E. A. Merritt, M. Ahn, C. Roach, Z. Hou, C. L. M. J. Verlinde, W. G. J. Hol, E. Fan, *J. Am. Chem. Soc.* **2002**, *124*, 12991–12998.
- [24] A. V. Pukin, C. A. G. M. Weijers, B. van Lagen, R. Wechselberger, B. Sun, M. Gilbert, M.-F. Karwaski, D. E. A. Florack, B. C. Jacobs, A. P. Tio-Gillen, A. van Belkum, H. P. Endtz, G. M. Visser, H. Zuilhof, *Carbohydr. Res.* **2008**, *343*, 636–650.
- [25] A. Holmner, G. Askarieh, M. Okvist, U. Krengel, *J. Mol. Biol.* **2007**, *371*, 754–764.
- [26] S. Fukuta, J. L. Magnani, E. M. Twiddy, R. K. Holmes, V. Ginsburg, *Infect. Immun.* **1988**, *56*, 1748–1753.
- [27] W. B. Turnbull, B. L. Precious, S. W. Homans, *J. Am. Chem. Soc.* **2004**, *126*, 1047–1054.
- [28] T. K. Dam, C. F. Brewer, *Chem. Rev.* **2002**, *102*, 387–429.
- [29] J. Lebowitz, M. S. Lewis, P. Schuck, *Protein Sci.* **2002**, *11*, 2067–2079.
- [30] P. Schuck, M. A. Perugini, N. R. Gonzales, G. J. Howlett, D. Schubert, *Biophys. J.* **2002**, *82*, 1096–1111.
- [31] W. P. Jencks, *Proc. Natl. Acad. Sci. USA* **1981**, *78*, 4046–4050.
- [32] B. Bilgic, D. T. Moustakas, G. M. Whitesides, *J. Am. Chem. Soc.* **2007**, *129*, 3722–3728.
- [33] J. Liu, Z. Zhang, X. Tan, W. G. J. Hol, C. L. M. J. Verlinde, E. Fan, *J. Am. Chem. Soc.* **2005**, *127*, 2044–2045.
- [34] P. I. Kitov, T. Lipinski, E. Paszkiewicz, D. Solomon, J. M. Sadowska, G. A. Grant, G. L. Mulvey, E. N. Kitova, J. S. Klassen, G. D. Armstrong, D. R. Bundle, *Angew. Chem.* **2008**, *120*, 684–688; *Angew. Chem. Int. Ed.* **2008**, *47*, 672–676.
- [35] J. Mou, J. Yang, Z. Shao, *J. Mol. Biol.* **1995**, *248*, 507–512.
- [36] R. Wang, J. Shi, A. N. Parikh, A. P. Shreve, L. Chen, B. I. Swanson, *Colloids Surf. B* **2004**, *33*, 45–51.
- [37] E. A. Merritt, S. Sarfaty, I. K. Feil, W. G. J. Hol, *Structure* **1997**, *5*, 1485–1499.
- [38] C. F. Brewer, *Lectins Biol. Biochem. Clin. Biochem.* **1997**, *11*, 10–16.
- [39] A. Imberty, M. Wimmerov, E. P. Mitchell, N. Gilboa-Garber, *Microbes Infect.* **2004**, *6*, 221–228.
- [40] Z. Zhang, J. C. Pickens, W. G. J. Hol, E. Fan, *Org. Lett.* **2004**, *6*, 1377–1380.
- [41] J. C. T. Carlson, S. S. Jena, M. Flenniken, T.-F. Chou, R. A. Siegel, C. R. Wagner, *J. Am. Chem. Soc.* **2006**, *128*, 7630–7638.
- [42] N. Dotan, D. Arad, F. Frolov, A. Freeman, *Angew. Chem.* **1999**, *111*, 2512–2515; *Angew. Chem. Int. Ed.* **1999**, *38*, 2363–2366.
- [43] P. Ringler, G. E. Schulz, *Science* **2003**, *302*, 106–109.
- [44] T. Amin, T. R. Hirst, *Protein Expression Purif.* **1994**, *5*, 198–204.
- [45] T. G. M. Lauterslager, D. E. A. Florack, T. J. van der Wal, J. W. Molthoff, J. P. M. Langeveld, D. Bosch, W. J. A. Boersma, L. A. T. Hilgers, *Vaccine* **2001**, *19*, 2749–2755.
- [46] L. M. Schwartz, *Anal. Chem.* **1975**, *47*, 963–964.
- [47] H. Durchschlag, P. Zipper in *Analytical Ultracentrifugation Techniques and Methods* (Eds.: D. J. Scott, S. E. Harding, A. J. Rowe), Royal Society of Chemistry, Cambridge, **2005**, pp. 389–431.
- [48] P. Schuck, *Biophys. J.* **2000**, *78*, 1606–1619.

Received: August 17, 2008

Published online on November 25, 2008